Electrons and Positron Spectra Measured by the PAMELA Space Experiment

EMILIANO MOCCHIUTTI[1] ON BEHALF OF THE PAMELA COLLABORATION
[1] *INFN, Sezione di Trieste, Padriciano 99, I–34149 Trieste, Italy*
Emiliano.Mocchiutti@ts.infn.it

Abstract: PAMELA is a satellite borne experiment designed to study with great accuracy cosmic rays in a wide energy range. The study of the antimatter component is one of PAMELA's main objectives. The experiment, housed on board the Russian Resurs–DK1 satellite, was launched on June 15th 2006 in a 350 – 600 km orbit with an inclination of 70 degrees. In this work we present the measurement of galactic electron and positron spectra in the energy range between 1 GeV and few hundred GeV.

Keywords: PAMELA, Cosmic rays, electrons, positrons.

1 Introduction

PAMELA is a dedicated satellite borne experiment conceived by the WiZard collaboration to study the anti–particle component of the cosmic radiation. In this work we describe the scientific objectives, the detector and the results of PAMELA in the measurement of galactic electrons and positrons after five years of data taking.

2 Physics goals and instrument description

The PAMELA physics goal is the precise measurement of the cosmic ray composition at 1 Astronomical Unit (AU). PAMELA has been mainly conceived to perform high–precision spectral measurement of antiprotons and positrons and to search for antinuclei, over a wide energy range. Besides the study of cosmic antimatter, the instrument setup and the flight characteristics allow many additional scientific goals to be pursued [1].

The instrument is installed inside a pressurized container attached to the Russian Resurs–DK1 satellite that was launched into Earth orbit by a Soyuz–U rocket on June 15th 2006 from the Baikonur cosmodrome in Kazakhstan. The mission is foreseen to last till at least December 2011.

A schematic overview of the PAMELA apparatus is shown in fig. 1. It comprises the following subdetectors, arranged as shown in figure, from top to bottom: a time–of–flight system (TOF – S1, S2, S3); a magnetic spectrometer; an anticoincidence system (AC – CARD, CAT, CAS); an electromagnetic imaging calorimeter; a shower tail catcher scintillator (S4) and a neutron detector.

Planes of plastic scintillator mounted above and below the spectrometer form the TOF system. Its timing resolution allows albedo–particle identification and mass discrimination below 1 GeV/c. The TOF provides also a fast signal for triggering the data acquisition

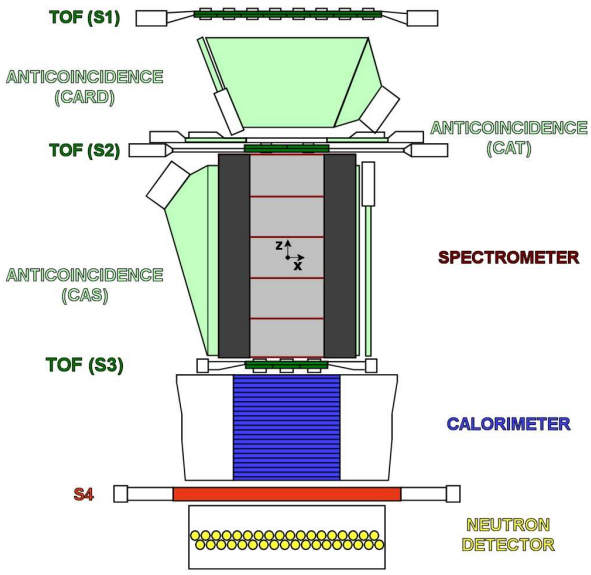

Figure 1: A schematic view of the PAMELA apparatus. Magnetic field lines are oriented parallel to the y direction.

The central components of PAMELA are a permanent magnet and a tracking system composed of six planes of double–sided silicon sensors, which form the magnetic spectrometer. This device is used to determine the rigidity (momentum divided by charge) and the charge of particles crossing the magnetic cavity. The rigidity measurement is done through the reconstruction of the trajectory

based on the impact points on the tracking planes and the resulting determination of the curvature due to the Lorentz force. The direction of bending of the particle (*i.e.* the discrimination of the charge sign) is the key method used to separate matter from anti–matter. The magnetic field of the spectrometer of PAMELA is generated by a permanent magnet composed of five identical modules placed one on top of another to form a 43.6 cm high tower. The acceptance of the spectrometer, which also defines the overall acceptance of the PAMELA experiment, is 21.5 cm^2sr and the spatial resolution of the tracking system is better than 4 μm up to a zenith angle of 10°, corresponding to a maximum detectable rigidity exceeding 1 TV.

The spectrometer is surrounded by a plastic scintillator veto shield, aiming to identify false triggers and multiparticle events generated by secondary particles produced in the apparatus.

The sampling imaging calorimeter (16.3 X_0, 0.6 λ_0) is mounted below the spectrometer and it comprises 44 single–sided silicon strip detector planes interleaved with 22 plates of tungsten absorber. The high granularity of the calorimeter and the use of silicon strip detectors provide detailed information on the longitudinal and lateral profiles of particles' interactions as well as a measure of the deposited energy. The main task of the calorimeter is to select positrons and antiprotons from the large background constituted by protons and electrons, respectively. Positrons have to be identified from a background of protons that is about 10^3 times the positrons component at 1 GeV/c, increasing to 5×10^3 at 10 GeV/c. Antiprotons have to be selected from a background of electrons that decreases from 5×10^3 times the antiproton component at 1 GeV/c to less than 10^2 times above 10 GeV/c. This means that PAMELA must be able to separate electrons from hadrons at a level better than 10^5. Much of this rejection power in PAMELA is provided by the calorimeter. Besides the electron-hadron separation, the calorimeter directly measure the energy of electrons and positrons.

A plastic scintillator system mounted beneath the calorimeter aids the identification of high–energy electrons and is followed by a neutron detection system for the selection of high–energy electrons which shower in the calorimeter. More technical details about the entire PAMELA instrument and launch preparations can be found in [2].

2.1 Negative electron spectrum

As it will be discussed in section 2.2, the rise in the positron fraction measured by PAMELA could be due to a very soft electron (e^-) spectrum. It is therefore important to precisely measure the negative electron spectrum in order to put constraints in the interpretation of the positron fraction rise. Moreover, if a primary positron source exists, it is difficult to explain the generation and acceleration of positrons without generating and accelerating the same amount of electrons. This implies that a negative electron spectrum measurement with high enough statistic and precision should reveal spectral features in the same energy range at which the positron fraction seems to deviate from the expected background.

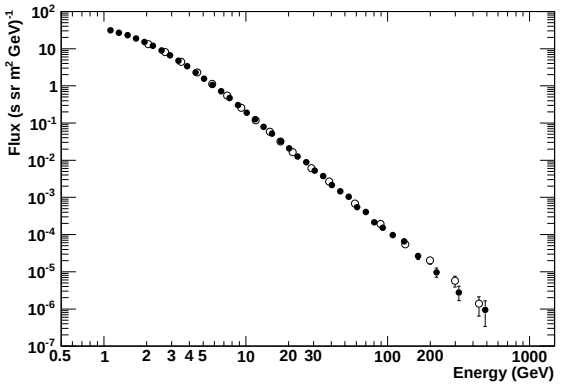

Figure 2: Electron flux as measured with PAMELA: comparison between the energy spectrum obtained using the spectrometer (closed circles) and the same using the calorimeter (open circles) to determine the energy of the events.

The PAMELA apparatus is able to separate negative electrons from positrons up to about 600 GeV [3]. The capabilities of the PAMELA detector allow also any systematic effect due to the energy measurement to be constrained and estimated accurately. In fact the energy of electrons can be determined using two independent detectors: the spectrometer and the electromagnetic calorimeter. Fig. 2 shows the negative electron spectrum as measured by PAMELA. Both the presented fluxes have been obtained selecting negative particles with the spectrometer; the energy measurement and binning is different and is performed using the tracking system (full circles) or the calorimeter (open circles). In the case of the calorimeter energy determination, in order to minimize the transversal leakage, strong containment conditions are required. This reduces the statistics of the sample. Longitudinal leakage is taken into account by fitting the shower longitudinal profile with a gamma function. With these conditions a precise energy measurement is achieved. As can be seen from the figure the resulting flux are in very good agreement and the comparison between the two fluxes can be used to set a 2% systematic error in the negative electron spectrum measurement.

Fig. 3 shows the PAMELA results [3] compared to other recent experimental measurements data [4, 5, 6, 7, 8, 9, 10, 11, 12]. The data from [8, 9, 10, 11, 12] and the highest data point from HEAT [6] refer to the sum of electron and positron fluxes. Considering statistical and systematic uncertainties, no significant disagreements are found between PAMELA and the recent ATIC [10] and Fermi [12] data, even considering an additional positron component in these measurements of order a few percent (see [13]).

The overall results can be easily described by a single power law, however a certain hardening of the PAMELA

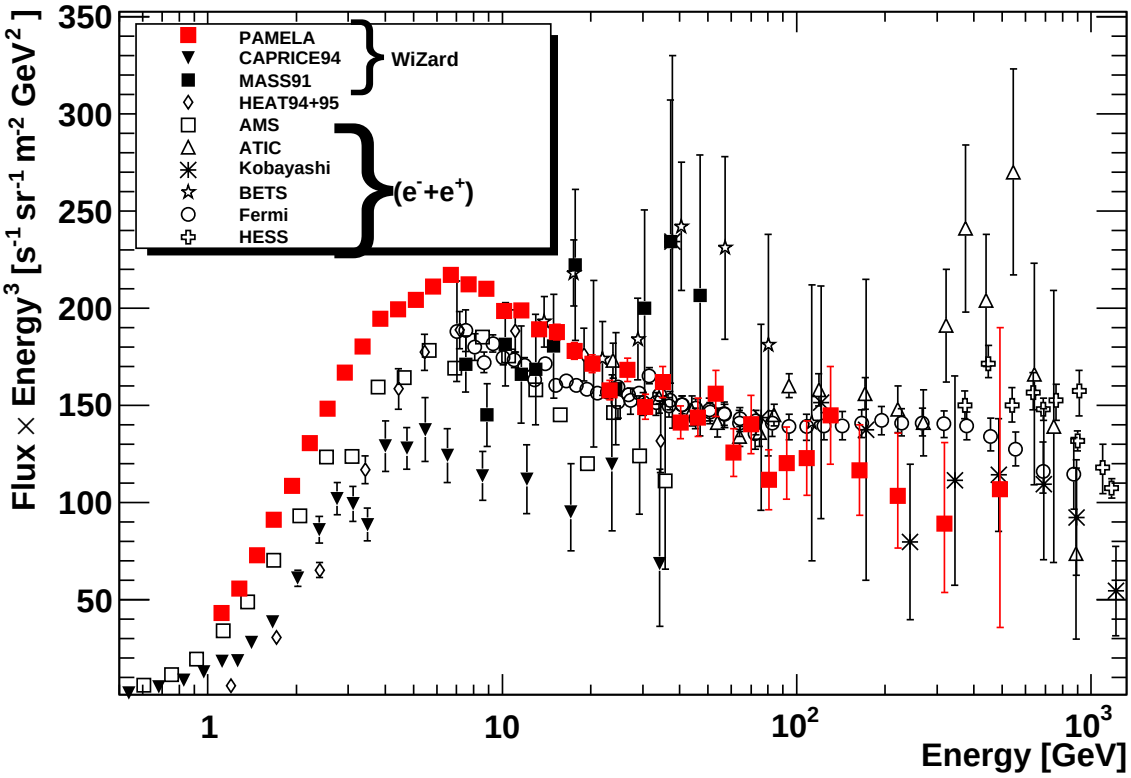

Figure 3: Electron flux as measured with PAMELA compared to results from other experimental data.

spectrum may be present at high energies. This possible break in the spectrum seems to be in agreement with the rise in the positron fraction.

2.2 Positron fraction

Protons are the main source of background in the positron sample and an excellent positron identification is needed to reduce the contamination at a negligible level.

The proton background estimation method has been used to obtain the published results [13, 14]. This approach consists in keeping a very high selection efficiency and in quantifying the residual proton contamination by the mean of a so–called "spectral analysis". The proton distributions needed to estimate the contamination is obtained in a conservative approach using the flight calorimeter data without any dependence on simulations or test beam data. For this purpose, the calorimeter is divided in an upper ("pre–sampler") and a lower part. The upper part, made of two tungsten planes and four detector planes, is used to reject non–interacting particles, and the lower part consisting in 20 tungsten planes and 40 detector planes is used to evaluate the calorimeter variables. The sample of events passing the non-interacting condition in the first part is a nearly pure sample of protons with a positron contamination of less than 2% at rigidities greater than 1.5 GV. For those events, calorimeter variables are evaluated in the lower part and the distribution of the lateral shower spread for protons have been obtained. Positive and negative samples are selected using only the first 40 sensitive planes of the calorimeter, to have observables comparable to the ones constructed for protons with the lower 40 planes of the calorimeter. The negative events are electrons with a negligible contamination of other particles. The number of positrons is estimated from the positive sample after subtracting the proton background.

The positron fraction results are shown in fig. 4 where PAMELA data [13, 14] are compared to some recent measurements ([4, 5, 15, 16, 17, 18, 19, 20, 21]) and to the standard model theoretical prediction for secondary positron production. At low energy PAMELA data are lower than most of the other data and this can be interpreted as an observation of charge–sign dependent solar modulation effects. Between about 6 and 10 GeV the PAMELA positron fraction is compatible with other measurements and above 10 GeV it increases significantly with energy. The PAMELA data cannot be described by the standard model of secondary production, black line in fig. 4. The secondary production model has its indetermination due to the knowledge of the fluxes of primary particles, of the interaction cross–sections, of the average amount of traversed matter, and of the electron spectrum. However the rising at

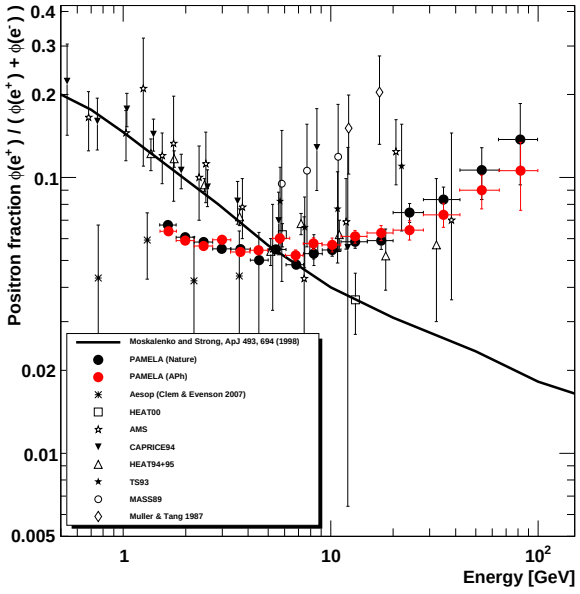

Figure 4: The PAMELA positron fraction compared to other experimental results and the standard model prediction for secondary positron production.

E>10 GeV seems a very difficult feature to be reproduced by a pure secondary component without using an unrealistic soft electron spectrum and ad hoc tuning of the other parameters [22], suggesting the existence of other primary sources [23].

Many explanations about the origin of the positron excess have been postulated. These models can be divided in terms of astrophysical sources, like pulsars [24] or the distribution of Supernovæ remnants [25] in the Galaxy, or more speculative ones, like annihilation of new type of dark matter [26] or of the lightest superparticle dark matter [27].

The measurement of the PAMELA positron flux will be presented at the conference.

3 Conclusions

PAMELA is continuously taking data and the mission is planned to continue until at least December 2011. The increase in statistics will allow higher energies to be studied. An analysis for positron flux till low energy (down to 100 MeV), and primary cosmic rays nuclei is in progress and will be the topic of future publications.

Acknowledgment

We would like to acknowledge contributions and support from: Italian Space Agency (ASI), Deutsches Zentrum für Luft– und Raumfahrt (DLR), The Swedish National Space Board, Swedish Research Council, Russian Space Agency (Roskosmos, RKA). R. S. wishes to thank the TRIL program of the International Center of Theoretical Physics, Trieste, Italy that partly sponsored his activity.

References

[1] Picozza P. *et al.*, *Proceedings of 20th ECRS, Lisbon – Portugal 2006.*
[2] Picozza P. *et al.*, Astrophys. J., **27** (2007), 296.
[3] Adriani O. *et al.*, Phys. Rev. Lett., **106** (2011), 201101.
[4] Boezio M. *et al.*, Astrophys. J., **532** (2000) 653.
[5] Alcaraz J. *et al.*, Phys. Lett. B, **484** (2000) 10.
[6] DuVernois M. A. *et al.*, Astrophys. J., **559** (2001), 296.
[7] Grimani C. *et al.*, Astron. Astrophys., **392** (2002), 287.
[8] Kobayashi T.*et al.*, *Proc. 26th Int. Cosmic Ray Conf. (Salt Lake City)*, **3** (1999), 61.
[9] Torii S. *et al.*, Astrophys. J., **559** (2001), 973.
[10] Chang J. *et al.*, Nature, **456** (2008), 362.
[11] Aharonian F. *et al.*, Phys. Rev. Lett., **101** (2008), 261104.
[12] Ackermann M. *et al.*, Phys. Rev. D, **82** (2010), 092004.
[13] Adriani O. *et al.*, Astropart. Phys., **34** (2010) 1.
[14] Adriani O. *et al.*, Nature, **458** (2009) 607.
[15] Golden R. L. *et al.*, Astrophys. J., **436** (1994) 769.
[16] Beatty J. J. *et al.*, Phys. Rev. Lett., **93** (2004) 241102.
[17] Barwick S. W. *et al.*, Astrophys. J., **482** (1997) L191.
[18] Gast H.,Olzem J. and Schael S., *Proceeding of XLI Rencontres de Moriond, Electroweak Interaction and Unified Theories, La Thuile, Italy*, 2006, p. 421.
[19] Clem J. and Evenson P., *Proceedings of 30th International Cosmic Ray Conference, Merida – Mexico 2006*, edited by Caballero R., D'Olivo J. C., Medina–Tanco G. and Valdés–Galicia J. F. (Universidad Nacional Autónoma de México, Mexico City, Mexico) 2008, vol. 6 p. 27.
[20] Müller D. and Tang K. K., Astrophys. J., **312** (1987) 183.
[21] Moskalenko I. and Strong A., Astrophys. J., **493** (1998) 694.
[22] Delahaye T., Donato F., Fornengo N., Lavalle J., Lineros R., Salati P. and Taillet R., astro–ph/0809.5268 preprint (2008).
[23] Serpico P. D., Phys. Rev. D, **79** (2009) 021302.
[24] Yuksel H., Kistler M. D. and Stanev T., astro–ph/0810.2784 preprint (2008).
[25] Shaviv N. J., Nakar E. and Piran T., astro–ph/0902.0376 preprint (2009).
[26] Hooper D. and Profumo S., Phys. Reports, **453** (2007) 29.
[27] Grajek P. *et al.*, astro–ph/0812.4555 preprint (2008).